LEGIBILITY NOTICE

A major purpose of the Technical Information Center is to provide the broadest dissemination possible of information contained in DOE's Research and Development Reports to business, industry, the academic community, and federal, state and local governments.

Although a small portion of this report is not reproducible, it is being made available to expedite the availability of information on the research discussed herein.

LA-UR -89-1966

Los Alamos National Laboratory is operated by the University of California for the United States Department of Energy under contract W-7405-ENG-36.

LA-UR--89-1966

DE89 014256

TITLE: NEUTRINO PHYSICS AT LAMPF

AUTHOR(S): Gerald T(homas) GARVEY

SUBMITTED TO: To be published in Proceedings of
XXIII Yamada Conferernce on Nuclear Weak
Process and Nuclear Structure
June 12-15, 1989

DISCLAIMER

Los Alamos Los Alamos National Laboratory
Los Alamos, New Mexico 87545

NEUTRINO PHYSICS AT LAMPF

G. T. Garvey
Los Alamos National Laboratory, Los Alamos, NM 87545, U.S.A.

There are three neutrino experiments at LAMPF in various stages of completion or development. E225,[1] the study of electron-neutrino electron scattering, which completed data taking in December 1986 and has just about completed all its analysis. E645,[2] a search for $\bar{\nu}_\mu \rightarrow \bar{\nu}_e$ oscillation, is in its third and final year of data taking. The Large Čerenkov Detector (LCD), associated with E1015,[3] has undergone extensive scientific and technical review and we are presently trying to obtain the necessary funds to build the detector, beam line, and target. In the following, each of these experiments will be briefly discussed. Before doing so, it is useful to show the characteristics of the neutrino spectrum resulting from the decay of π^+ at rest. This spectrum is shown in Fig. 1. It is also useful to realize that, on average, an 800-MeV proton from LAMPF produces about 0.1 π^+ decaying at rest.

E225

The purpose of E225 is to measure the $\nu_e + e^- \rightarrow \nu_e + e^-$ elastic scattering cross section. This process is of great interest because it provides a unique opportunity to measure the interference between $W^\pm$ and Z^0 exchange. The Standard Model (SM) predicts this interference is destructive and this experiment tests that prediction.

The detector is located 9.0 m from the LAMPF beam stop at 90° to the proton beam direction. The neutrinos seen by the experiment result from the decay of π^+ at rest, as the π^- mesons are absorbed in the stopping material. The ν_μ and $\bar{\nu}_\mu$ can scatter off electrons only via Z_0 exchange and hence are expected to have cross sections nearly 10 times smaller than the ν_e. Further, their cross section, (ν_μ, e) and $(\bar{\nu}_\mu, e)$, has been measured at higher energies[4,5] and these results can be directly used to subtract their yield, because of the point-like nature of the interacting particles.

The neutrino detector, shown in Fig. 2, has a total mass of 14 tons and is shielded from the production target by 6.5 m of Fe. The detector is a sandwich structure of forty layers. Each layer consists of a plane of plastic scintillator (NE114) 2.54 cm thick and 10 planes of polypropylene flash tubes for directional tracking alternating between vertical

and horizontal orientation. The scintillator plane is made up of four 2.54-cm × 76-cm × 305-cm pieces, each with a single 12.7-cm diameter PMT (RCA4525). These detectors produce a yield of 14 photoelectrons per MeV of energy loss. The flash tubes are 0.5 × 0.6 × 305 cm^3, which require 5200 per layer, or a total of 208,000 flash tubes for the entire detector. The efficiency of a tube was typically 0.6 and the tracking system had an angular resolution of ±7°. There is a complete description[6] of the detector in the literature.

One of the problems in carrying out neutrino experiments at LAMPF is the rather long duty factor (6–10%) of the linac and the resulting background due to cosmic rays. In E225 the cosmic rays are dealt with by 900-g/cm^2 shield of passive iron and four layers of active multiwire proportional chambers (MWPC) that cover all inner surfaces of the passive shielding. The floor has a single layer of MWPC. These MWPC provide a prompt veto that reduces the on-line trigger rate by a factor of 10^4 and identifies cosmic-ray muons for off-line analysis. The event trigger is derived from an energy signal above threshold ($1 \leq S \leq 16$ MeV) in three successive scintillator planes. Employing a 20-μs veto for each entering muon generates a dead time of 15% and reduced the residual cosmic-ray trigger rate to 0.1 Hz. The beam-associated trigger rate was 0.0025 Hz at 600 μA at E_p = 765 MeV.†

Figure 3(a) shows the observed spectrum while the beam is on as a function of the electron angle measured with respect to the incident ν direction. Cosmic-ray background is recorded while the beam is off and Fig. 3(b) shows the spectrum with cosmic-ray background subtracted. The cosmic-ray events are expected to produce an isotropic distribution. The peaking toward $\cos\theta = 1$ reflects the biased acceptance of the detector, which requires energy deposition in three successive scintillator planes. The electrons resulting from ν-e scattering are strongly forward peaked due to kinematics. The electron angular distribution in the lab is very forward peaked, particularly if an energy threshold is required for the detected electron. For $E_e > 10$ MeV, all events occur forward of 15° ($\cos 15° = 0.966$). The forward peak seen in the spectrum clearly corresponds to ν-e scattering. The more isotropic backgrounds seen in Fig. 3(b) arise principally from $\nu_e + {}^{12}C \rightarrow e^- + X$ and neutron-induced events that simulate electron-like events.

The spectra of n-p events as a function of (θ, E_{vis}) is obtained by determining the (θ, E_{vis}) event distribution that fails the tracking requirement because the events are n-p knock-ons. There are small amounts of ^{13}C, ^{27}Al, and Cl also present that would generate a predictable distribution in (θ, E_{vis}). A fit to the observed distribution yields the results shown in Table I.

The total number of νe events must have the $\nu_\mu e$ and $\bar{\nu}_\mu e$ events subtracted to obtain the $\nu_e e$ yield. This is done by using the $\nu_\mu e$ and $\bar{\nu}_\mu e$ cross section measured at AGS[4] and CERN[5] to yield

$$\nu e - \nu_\mu e - \bar{\nu}_\mu e - \nu_e e = 234 \pm 35 \ .$$

† The beam is degraded from the nominal 800-MeV 1-mA beam because it passes through two pion production targets before being transported to the beam stop.

Table I. Allocation of Events in E225.

Process	Number of Events
$\nu + e$	295 ± 35
$\nu_e + {}^{12}C \rightarrow e^- + X$	626 ± 71
$\nu_e + {}^{13}C, {}^{27}Al, {}^{35}C \rightarrow e^- + X'$	136 ± 102
n-p events	435 ± 90
Total	1492

The number of μ^+ created by incident 700–800-MeV protons has been recently remeasured[7] at LAMPF and is in agreement with earlier measurements.[8] Using this information, along with the measured efficiency of the detector ($\epsilon = 0.165$), one finds

$$\sigma(\nu_e, e^-) = (9.89 \pm 1.48 \pm 0.99) \times 10^{-45} \text{ cm}^2 \text{ MeV}^-$$

in good agreement with the SM prediction of 9.5×10^{-45} cm^2 MeV$^-$ for $\sin^2\theta_W = 0.23$. Alternatively, if one assumes destructive interference and uses the experimental[4,5] values for $\nu_\mu e$ and $\bar{\nu}_\mu e$, the observed yield in E225 yields $\sin^2\theta_W = 0.235 \pm 0.046 \pm 0.035$.

E225 has the capability to record subsequent activity in the detector for times up to 64 ms after an event trigger via the use of a 60-KH clock. The clock time is recorded with the subsequent event. Using this capability, the beta decay associated with $^{12}C(\nu_e, e)^{12}N$(g.s.), which has a half life of 15.9 ms and an endpoint energy of 15 MeV, has been detected. Figure 4 shows the decay curves recorded for beam-on and beam-off events. The ^{12}N decay can be extracted and a cross section determined for the incident ν_e spectra of

$$\sigma[^{12}C(\nu_e, e^-)^{12}N(\text{g.s.})] = 1.0 \pm 0.11 \pm 0.13 \times 10^{-41} \text{ cm}^2 \ .$$

This is in excellent agreement with a very reliable prediction,[9] based on ^{12}N beta decay and ^{12}C μ^- capture rates of

$$\sigma_{\text{p-ed}}[^{12}C(\nu_e, e^-)^{12}N(\text{g.s.})] = 0.94 \times 10^{-41} \text{ cm}^2 \ .$$

E645

E645 is a neutrino oscillation appearance experiment that takes advantage of the fact that there is no $\bar{\nu}_e$ in the neutrino spectrum resulting from the decay of stopped pions (π^+ only). The $\bar{\nu}_e$ suppression at the LAMPF beam stop has been estimated at 1.4×10^{-4}. Therefore a sensitive experiment can be devised based on the reaction

$$\bar{\nu}_e + p \rightarrow e^+ + n \qquad (1)$$

to search for an oscillation of $\bar{\nu}_\mu$, say into $\bar{\nu}_e$. Under the assumption that the oscillation involves only two neutrino species, the probability of neutrino species ν_1 changing into

neutrino species ν_2 is

$$P(\nu_1 \rightarrow \nu_2) = \sin^2 2\theta \sin^2 \left(1.27\Delta m^2 \frac{L}{E}\right) \quad , \tag{2}$$

where θ is the mixing angle between types 1 and 2, Δm^2 is the difference in the square of these masses, L (in meters) is the distance traversed by the neutrino, and E (MeV) is the neutrino energy.

In this experiment, the detector is 26.8 m from the beam stop and at 9° to the incident proton beam direction. The detector (Fig. 5) is again a fine-grained sandwich-type consisting of 40 planes of liquid scintillator backed by 41 planes of vertical and horizontal pairs of proportional drift tubes (PDT).

The liquid scintillator employed is mineral oil doped with pseudocumene. It is contained in cells 30 cm × 366 cm × 3 cm, with twelve cells constituting a plane 360 cm × 366 cm. Each cell was viewed by a PMT at each end. A plane of PDT's consists of 45 cells, each 7 cm × 366 cm × 3 cm. The detector has a total mass of 20 tons. The trigger is a hit in three of any four successive scintillator planes. The trigger rate is ~0.53 Hz.

An interesting feature of this detector is the shield[10] that surrounds the detector on all sides. The shield design is highly redundant with 12.7-cm diameter phototubes on a 1-m^2 spacing that view a 15.24-cm deep layer of liquid scintillator designed to surround the detector. The detector is mounted on a cart that also carries a floor and back wall of veto scintillator. The cart fits into a movable cylindrical cosmic-ray shield of scintillator that surrounds the detector, as shown in Fig. 5. The 15.24-cm depth of veto liquid scintillator is very important in that a through-going muon loses some 30 MeV; hence, the threshold for events from the veto shield can be set well above background radiation levels and unnecessary dead time is avoided. The shield provides a 10^{-4} rejection on line and a better than 3×10^{-6} rejection level off line.

Each detector plane also has a very thin layer of gadolidium spray painted onto mylar sheets to detect the neutrons produced in Eq. (1). The capture of the thermalized neutrons on gadolidium is detected by prompt coincident signals due to the gadolidium capturing gamma rays in at least two of the scintillators for a period extending up to 107 μs subsequent to an event trigger. The electronics was designed to read out the activity in the detector and active shield from 53 μs before a trigger to 107 μs after the trigger. The efficiency of this mode of neutron detection was calculated to be 0.36. Good agreement[11] for the efficiency was found between a Monte Carlo calculation and measurements using tagged neutrons generated by the fission of ^{252}Cf. The detector and shield are placed in a tunnel with 2000 g/cm^2 overburden and an 8-m thick water plug is placed at the entrance to the tunnel.

Data are recorded during the 780-μs long beam pulses. Cosmic-ray backgrounds are recorded over a 1885-μs period before and a 978-μs period after the beam pulse.

The great majority of triggers are due to cosmic-ray events. They are of three types, electrons from stopping muons, through-going muons, and low-energy nontracking debris. The fine-grained nature of the detector serves to identify electrons very well. Figure 6

shows a plot of particle range vs visible energy deposited in the scintillator for contained tracks. Protons and electrons are seen to be well separated and protons can be rejected to a level of 10^{-3}. The cluster of events in the lower left is due to electrons from stopped muons and their energy spectrum is shown in Fig. 7. It is seen to compare excellently to the Monte Carlo simulation. These events also serve to determine that the number of contained electron events surviving the analysis cuts is 0.42 ± 0.03. Table II shows the statistics for the 1987 and 1988 runs. The 1989 run is just underway.

Table II. E645 Statistics in 1987 and 1988.

	1987	1988
Beam-on live time (LD)†	75.22	63.19
Pre-beam live time (LD)	170.60	152.70
Post-beam live time (LD)	95.22	79.23
Ratio of beam-off/beam-on	3.52	3.67
Charge on target (Coulombs)	5100	4405
Average beam current (C/LD)	67.80	69.71
Trigger	1269639	731888
1st pass cuts	203708	127100
2nd pass cuts	3018	3454
Neutrino candidates	47	36

†LD = LAMPF Day = 5600 s.

Figure 8 shows the spectrum of excess events due to the beam (i.e., beam on–beam off) during the 1987 run. All of the events below 30 MeV are ascribable to ν_e ^{12}C or νe scattering. The limits obtained on $\sin^2 2\theta$ and Δm^2 are shown in Fig. 9.

An analysis[12] of the 1987 run using the neutron detection capability has been carried out. In spite of the low efficiency for neutron detection, it achieves similar limits to those shown in Fig. 8, as one is able to loosen up the software cuts on the electron identification. In this analysis one finds a beam excess of 12.2 ± 7.6 events without requiring neutron coincidence and 0.4 ± 3.2 requiring neutron coincidence. Running E645 through 1989 should improve the 1987 limits by a factor of 2.25.

One criticism of the above detector is its poor efficiency for events corresponding to Eq. (1). The charge-changing cross section is nearly isotropic and a sandwich-type detector has a strongly forward peaked acceptance. Hence the efficiency is $(0.33)_{trig} \times (0.42)_{anal}$ = 14%, which is rather low. A detector that does not suffer from this shortcoming is now under active discussion at LAMPF.

E1015

This experiment[13] is designed to employ the intense pulsed proton beam from the Los Alamos Proton Storage Ring[14] (PSR), along with a Large Čerenkov Detector (LCD) to measure $\sin^2\theta_W$ to better than 1% accuracy in νe scattering. The concept uses the short pulses from the PSR (0.27 μs) to separate in time the ν_μ from π^+ decay from the $\bar{\nu}_\mu$ and ν_e from μ^+ decay. Thus, the ratio

$$R = \frac{\sigma(\nu_\mu e)}{\sigma(\overline{\nu}_\mu e) + \sigma(\nu_e e)} = \frac{3}{4}\,\frac{1 - 4\sin^2\theta_W + \frac{16}{3}\sin^4\theta_W}{1 + 2\sin^2\theta_W + 8\sin^2\theta_W}$$

can be accurately measured to determine $\sin^2\theta_W$. An error in the measurement of R is related to the error in the determination of $\sin^2\theta_W$ by

$$\frac{\delta R}{R} = 2.08\left(\frac{\delta \sin^2\theta_W}{\sin^2\theta_W}\right)_{\sin^2\theta_W = 0.23} ;$$

hence, a 2% measurement of R gives $\sin^2\theta_W$ to 1%.

The value of $\sin^2\theta_W$ measured in any given experiment is effected by radiative corrections. The radiative corrections appropriate to ν scattering are shown in Fig. 10. A consistent renormalization framework has been developed by Sirlin[15] that takes α_e, m_Z, and τ_μ as the fundamental parameters of the theory. The remaining renormalized parameters are then derived from those parameters to one loop to order $0[G_\mu\alpha]$ and are thus gauge invariant. The above quantity R is thus increased from its "tree level" value by 3.6%. Deviations from this value would indicate a breakdown in the SM. Hence, this experiment, along with the expected precision measurements of the W and Z masses, provide a real test of the SM.

The necessary separation of the neutrino types is accomplished via pion production with the short intense proton pulses from the PSR. This ring is injected by a macropulse (750 μs) of 800-MeV H^- ions from the LAMPF linac. The accumulated beam is then extracted in a single turn, giving a pulse of 270 ns. Using this pulse to produce pions allows the separation in time of ν_μ neutrinos from π^+ decay from the $\overline{\nu}_\mu$ and ν_e due to μ^+ decay, as shown in Fig. 11. The PSR is designed to produce 100-μa at 12 Hz. It currently delivers 50 μa for the production of pulsed neutrons for condensed matter physics research. As LAMPF has unused acceleration capability, it is planned to simultaneously accelerate H^- with H^+ and provide 240 μA at 48 Hz to PSR for ν production.

To carry out a precision measurement, high statistics are required. The limiting yield in E1015 is the yield from the prompt component (ν_μ). To carry out the experiment in reasonable time, therefore, the detector needs to be very large. Hence, a water Čerenkov detector with an active volume of 7 kilotons of H_2O was selected. Figure 12 shows how the detector surrounds the production target in such a way as to avoid neutrinos produced by decay in flight. The Čerenkov light is detected by 1.2×10^4 10-in PMT's. Table III shows the expected daily event rates based on 100 μA of 800-MeV protons. Table IV shows the contributions to the systematic error in R. A major contribution[16] to the error is subtraction of the $\nu_e + {}^{16}O$ background from the $\nu_e e$ plus $\nu_\mu e$ scattering. Figure 13 shows a Monte Carlo calculation, including multiple scattering, of the expected angular distribution of events with a 10-MeV threshold on electron energy. The other major contribution to the systematic error is events generated by neutrons produced by the beam. The present plan has 7.5-m radius cylindrical Fe shielding which attenuates the neutron flux to the point that they produce only 0.7 ...ents/day. This issue is under study; increasing the shielding by 1 m adds 1M$ more cost for additional PMT's.

Table III. Summary of Event Rates.

Type of Event	#/day	#/day $\cos\theta > 0.76$	Sect.
All ν e scattering	112.0	106.5	12.8.1
ν_μe	12.0	11.3	12.8.1
ν_ee	87.3	82.5	12.8.1
$\overline{\nu}_\mu$e	13.6	12.8	12.8.1
Beam-induced background			
Neutron-induced gammas	4.1	0.49	7.10
Neutron-induced pions (prompt)	0.22	0.22	7.1.4
(delayed)	0.544	0.065	7.1.4
Neutrino-oxygen	331	22.2	12.8.3
Cosmic-ray-induced background (5-μs gate)			
Stopped muon decay			
Out of 5 σ "dead zone"	1.73	0.21	9.3
Decay after 30 μs	0.04	0.004	9.3
Interactions of throughgoing muons	2.5	0.25	9.4.1
Muon capture and beta decay			
^{16}N beta decay (7 s, 10.4 MeV)	0.9	0.09	9.4.2
^{12}B beta decay (27 μs, 14 MeV)	1.4	0.14	9.4.2
Gammas from showers	0.04	0.004	9.5.1
Neutrons from hadronic interactions	1.4	0.14	9.5.2

Table IV. Contribution to Systematic Errors in R.

	Cause	Error in %
1.	Decay in flight	0.12
2.	Cosmic rays	0.01
3.	ν_e - O	0.50
4.	Prompt γ and $\pi^\pm$ from n interactions	0.65
5.	Delayed e from n induced π^+ decay	0.01
6.	Measurement of PSR shape	0.15
7.	Systematic time shift	0.08
8.	Absolute threshold energy	0.40
9.	Nonuniform efficiency	0.10
	Total systematic error	0.94 (added in quadrature)
	Total statistical error	1.60
	Total error in R	1.86 (added in quadrature)
	Total error in $\sin^2\theta_W$	0.89

This experiment has been approved by the LAMPF PAC, and by Ad hoc committees of DOE for scientific and technical merit. The project is now awaiting funding. It takes three years to construct and at least two years of full running at 240 μA to get $\sin^2\theta_W$ to 1%. This work is performed under the auspices of the U.S. Department of Energy. I would like to express a genuine debt of gratitude to Herb Chen, who was a

major figure in establishing neutrino physics at LAMPF. His untimely death on November 7, 1987, saddened us all and deprived us of an outstanding physicist and remarkable person. I would also like to acknowledge very useful discussions with Bob Burman, Brian Fujikawa, and Vern Sandberg in preparing this document.

References

(1) E225—A Study of Neutrino Electron Elastic Scattering—University of California at Irvine, Los Alamos National Laboratory, University of Maryland.

(2) E645—A Search for Neutrino Oscillations at LAMPF—Argonne National Laboratory, California Institute of Technology, Lawrence Berkeley Laboratory, Los Alamos National Laboratory, Louisiana State University, The Ohio State University.

(3) E1015– A Precision Test of the Standard Model by Neutrino-Electron Scattering—University of California at Irvine, UCLA, University of California at Riverside, University of Colorado, CEBAF, Los Alamos National Laboratory, University of New Mexico, University of Pennsylvania, Temple University, College of William & Mary.

(4) K. Abe et al., *Phys. Rev. Lett.* **62**, 1709 (1989).

(5) C. Dorenborsch et al., *Z. Phys.* **C42**, 367 (1989).

(6) R. C. Allen et al., *Nucl. Instr. and Meth.* **A269**, 177 (1988).

(7) R. C. Allen et al., Los Alamos National Laboratory document LA-UR-89-1891 (1989) (to be published in *Nucl. Instr. and Meth.*).

(8) H. H. Chen et al., *Nucl. Instr. and Meth.* **160**, 393 (1979).

(9) W. Donnelly, private communication.

(10) J. J. Napolitano et al., *Nucl. Instr. and Meth.* **A274**, 152 (1989).

(11) B. Fujikawa, private communication, to be published.

(12) L. S. Durkin et al., *Phys. Rev. Lett.* **61**, 1811 (1988).

(13) R. C. Allen et al., Los Alamos National Laboratory document LA-11300-P, April 1988.

(14) G. P. Lawrence, in the Proceedings of the IEEE Particle Accelerator Conference, Washington, D.C., April 1987, Vol. 2 (1987) p. 825.

(15) A. Sirlin, *Phys. Rev.* **D29**, 89 (1980).

(16) W. C. Haxton, *Phys. Rev.* **D36**, 2283 (1987).

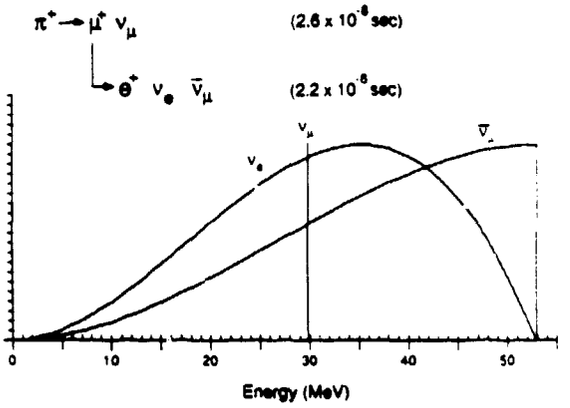
$\pi^+ \rightarrow \mu^+ \nu_\mu$ $(2.6 \times 10^{-8}$ sec)
$\hookrightarrow e^+ \nu_e \bar{\nu}_\mu$ $(2.2 \times 10^{-6}$ sec)
ν_μ
$\bar{\nu}_\mu$
ν_e
0
10
20
30
40
50
Energy (MeV)

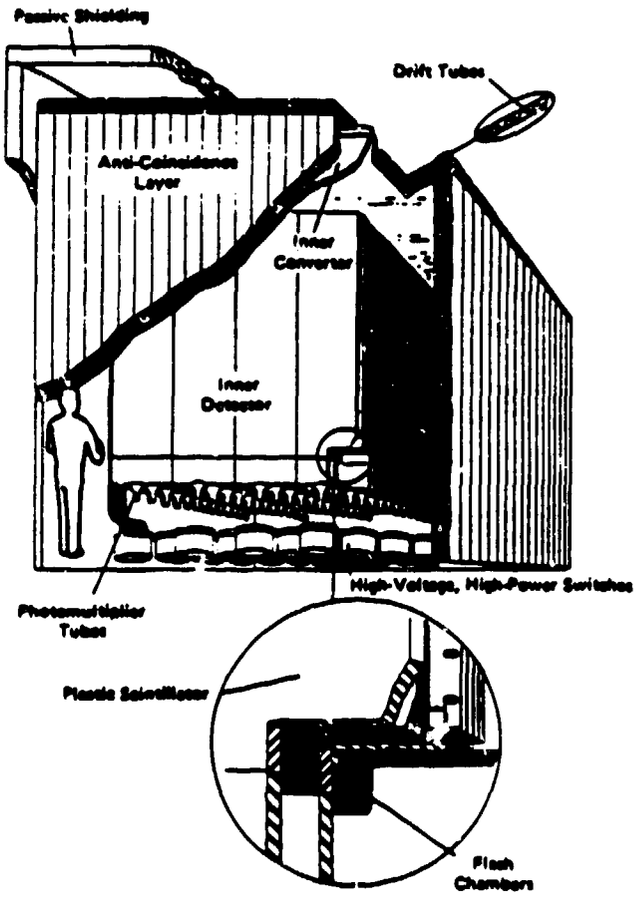
Passive Shielding
Drift Tubes
Anti-Coincidence Layer
Inner Converter
Inner Detector
High-Voltage, High-Power Switches
Photomultiplier Tubes
Plastic Scintillator
Flash Chambers

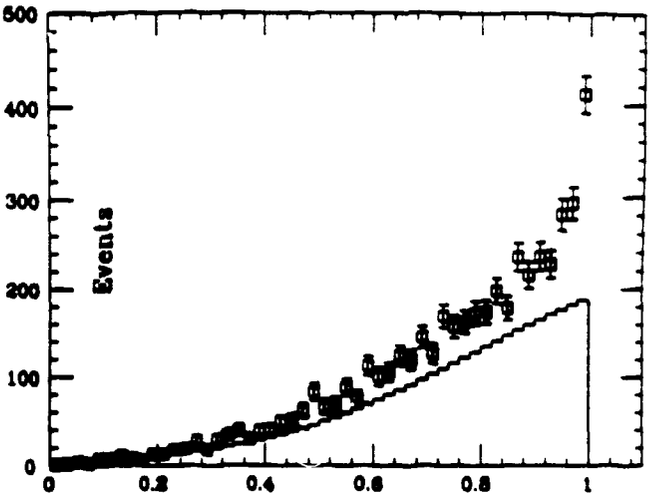
Events
cosine (θ_e)

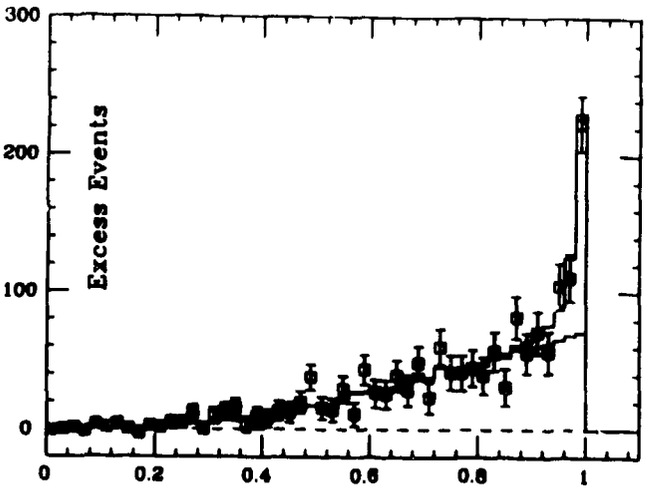
Excess Events
cosine (θ_e)

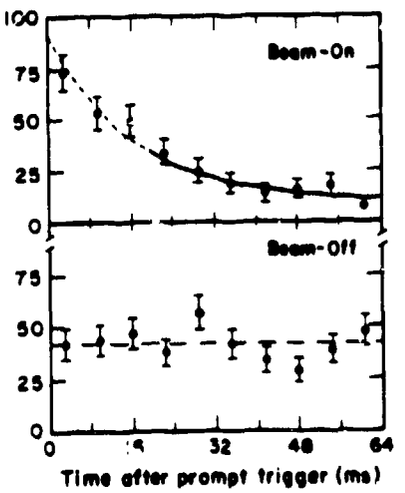
Beam-On
Beam-Off
Time after prompt trigger (ms)

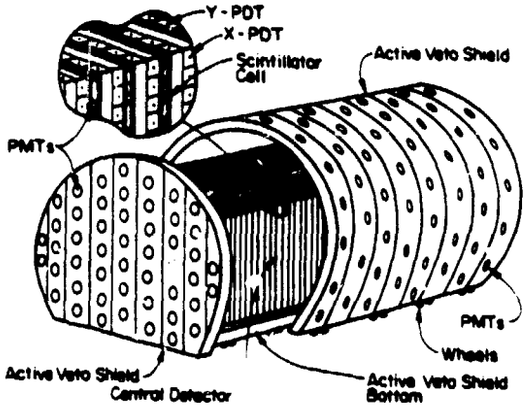
Y - PDT
X - PDT
Scintillator Cell
Active Veto Shield
PMTs
PMTs
Wheels
Active Veto Shield
Central Detector
Active Veto Shield
Bottom

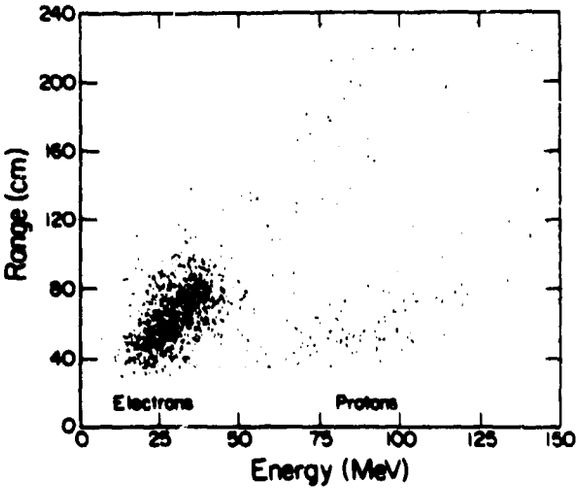
Range (cm)
Energy (MeV)
Electrons
Protons

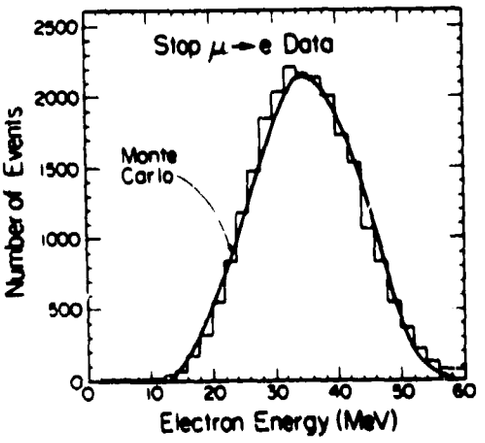
Stop μ → e Data
Number of Events
Monte Carlo
Electron Energy (MeV)

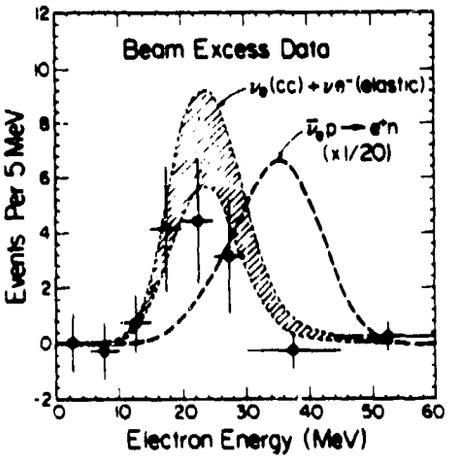
Beam Excess Data
Events Per 5 MeV
Electron Energy (MeV)
(x1/20)

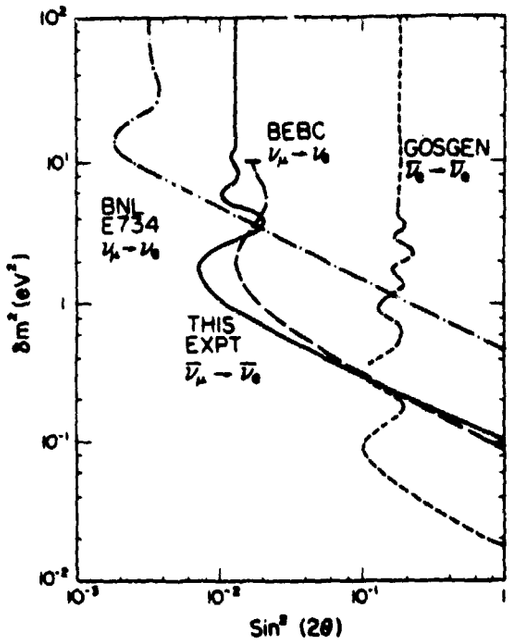
BEBC
$\nu_\mu - \nu_e$
GOSGEN
$\bar{\nu}_e - \bar{\nu}_e$
BNL
E734
$\nu_\mu - \nu_e$
THIS
EXPT
$\bar{\nu}_\mu - \bar{\nu}_e$
δm^2 (eV^2)
Sin^2 (2θ)

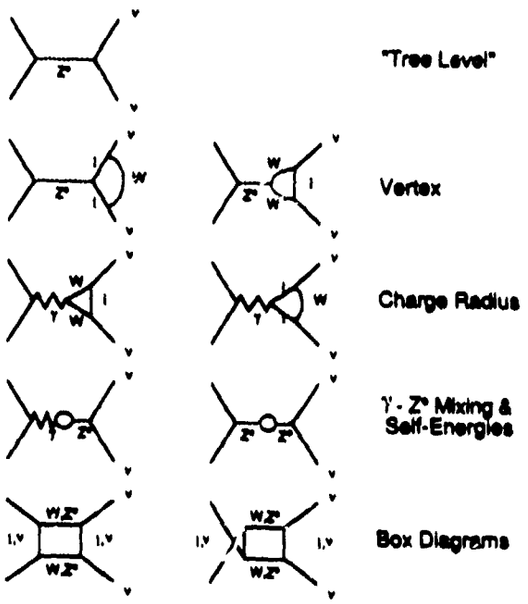
"Tree Level"
Vertex
Charge Radius
γ - Z^0 Mixing &
Self-Energies
Box Diagrams

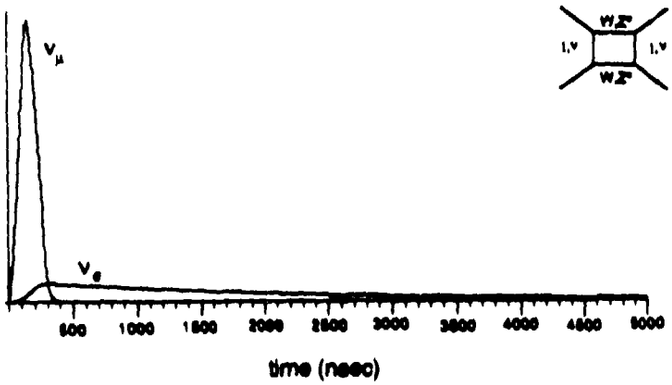
ν_μ
ν_e
time (nsec)

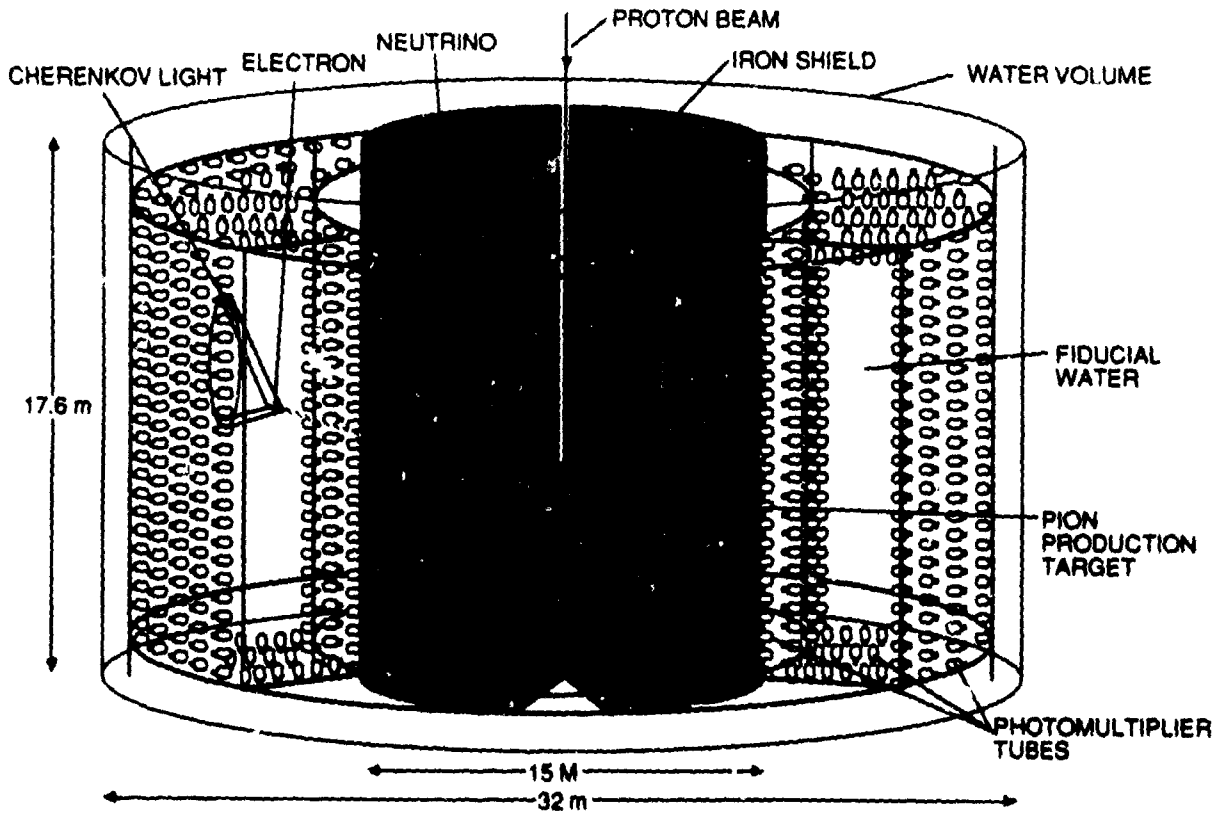
PROTON BEAM
NEUTRINO
ELECTRON
CHERENKOV LIGHT
IRON SHIELD
WATER VOLUME
17.6 m
FIDUCIAL WATER
PION PRODUCTION TARGET
PHOTOMULTIPLIER TUBES
15 M
32 m

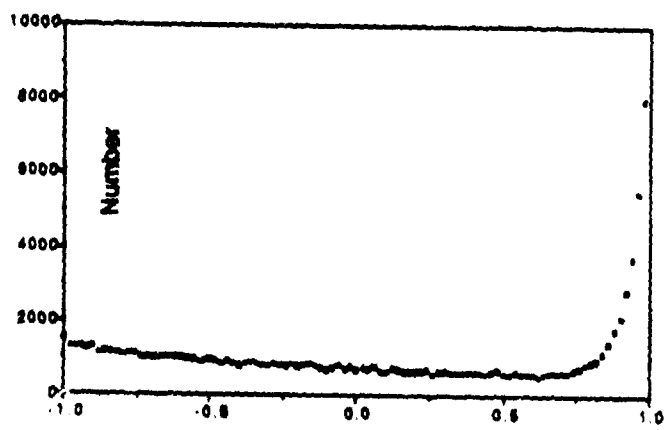
10000
8000
6000
4000
2000
0
Number
-1.0
-0.5
0.0
0.5
1.0
cos(Theta) Reconstructed